Strong enhancement of d-wave superconducting state in the three-band Hubbard model coupled to an apical oxygen phonon

Z. B. Huang,[1] H. Q. Lin,[2] and E. Arrigoni[3]
[1]*Faculty of Physics and Electronic Technology, Hubei University, Wuhan 430062, China*
[2]*Department of Physics, The Chinese University of Hong Kong, Hong Kong, China*
[3]*Institute of Theoretical and Computational Physics, Graz University of Technology, Petersgasse 16, A-8010 Graz, Austria*
(Received 18 November 2010; published 28 February 2011)

We study the hole binding energy and pairing correlations in the three-band Hubbard model coupled to an apical oxygen phonon, by exact diagonalization and constrained-path Monte Carlo simulations. In the physically relevant charge-transfer regime, we find that the hole binding energy is strongly enhanced by the electron-phonon interaction, which is due to a novel potential-energy-driven pairing mechanism involving reduction of both electronic potential energy and phonon related energy. The enhancement of hole binding energy, in combination with a phonon-induced increase of quasiparticle weight, leads to a dramatic enhancement of the long-range part of d-wave pairing correlations. Our results indicate that the apical oxygen phonon plays a significant role in the superconductivity of high-T_c cuprates.

DOI: 10.1103/PhysRevB.83.064521 PACS number(s): 74.20.−z, 71.10.Fd, 74.25.Kc, 74.72.−h

I. INTRODUCTION

Despite years of intensive research, the pairing mechanism responsible for d-wave superconductivity (dSC) in the high-T_c cuprates remains a puzzle. It is generally believed that the conventional phonon mechanism is inconsistent with d-wave pairing symmetry and not strong enough to explain transition temperatures higher than 100 K. Most investigations in this direction have been focused on the pure electronic mechanism, but no consensus has been reached so far. Recently, accurate experiments displayed pronounced phonon and electron lattice effects in these materials, which are manifested by a large softening and broadening of certain phonon modes in the whole doping region. In particular, the in-plane copper-oxygen bond-stretching phonon, apical oxygen phonon (AOP), and oxygen B_{1g} buckling phonon are shown to be strongly coupled to charge carriers.[1,2] Moreover, photoemission spectroscopy-resolved kink structures[3,4] are probably caused by coupling of quasiparticles to phonon modes. These findings suggest that phonons are important for the physical properties of high-T_c cuprates.

Various theoretical attempts have been made to understand the role of phonons in high-T_c superconductivity (HTSC),[5–8] but the answer remains unclear. In a functional renormalization-group study,[6] Honerkamp *et al.* found that the B_{1g} buckling phonon enhances the d-wave pairing instability in the Hubbard model. More recently, an exact-diagonalization (ED) study of the t-J model coupled to phonons shows that coupling to the buckling mode stabilizes d-wave pairing while coupling to the breathing mode favors a p-wave pairing.[7] On the other hand, based on dynamical cluster Monte Carlo calculations of the Hubbard model coupled to Holstein, buckling, and breathing phonons, Macridin *et al.* found that while these phonons can indeed enhance pairing, a strong phonon-induced reduction of quasiparticle weight leads to a suppression of dSC.[8]

In this paper, we study the effect of AOP on dSC in the more realistic three-band Hubbard model. Our work is motivated by recent experiments showing that the distance between apical oxygen and the CuO_2 plane,[9] the disorder around apical oxygen,[10,11] and the apical hole state[12] have significant effects on T_c. Basically, there are two routes for apical oxygen to affect HTSC: one is to tune the electronic structure of the CuO_2 plane, leading to a change of T_c;[13] the other one is to directly couple apical oxygen vibrations to charge carriers on the conducting CuO_2 plane.[14,15] Here we focus on the second route and study a strongly anharmonic vibration of apical oxygen in a double-well potential, which is evidenced in the x-ray-absorption spectroscopy of several typical high-T_c compounds.[16–18] For a strongly anharmonic motion in the double-well potential, the first excitation energy $\Delta E = E_1 - E_0$ is much smaller than the ones excited to higher energy levels $E_{n\geqslant 2}$. In this case one can take into account only the lowest quantum states Φ_0 and Φ_1 with energies E_0 and E_1 and model the low-energy motion of apical oxygen by a local two-level system represented by a pseudospin[19,20] degree of freedom.

Our main results, obtained by ED and constrained-path Monte Carlo (CPMC) methods, are presented in Figs. 1(b), 2(a), and 4. Figure 2(a) clearly shows that the coupling to the AOP induces a strong enhancement of hole binding energy, and this enhancement effect grows as the Coulomb repulsion U_d on the copper site is increased. An analysis of the contribution of different energies to the hole binding energy reveals a novel potential-energy-driven pairing mechanism that involves reduction of both electronic potential energy and phonon related energy. As a combination of increasing pairing interaction and quasiparticle weight [see Fig. 1(b)], the d-wave pairing correlations are found to be strongly enhanced by the electron-phonon (el-ph) coupling (see Fig. 4).

Our paper is organized as follows: In Sec. II, we define the Hamiltonian and the physical quantities calculated and discuss the choice of model parameters. In Sec. III, we present our numerical results and discuss the physical mechanism responsible for the AOP-induced enhancement of dSC. Finally, in Sec. IV, we discuss in detail our main conclusions.

II. MODEL AND NUMERICAL APPROACH

To model the electronic structure of CuO_2 plane and the coupling of holes to the anharmonic AOP, we adopt the following Hamiltonian proposed in Ref. 14:

$$H = H_k + H_{\rm pot} + H_{\rm ph}, \tag{1}$$

where H_k, $H_{\rm pot}$, and $H_{\rm ph}$ stand for the kinetic motion of holes, the potential energy for holes, and phonon related energy, respectively. They are expressed in the form

$$H_k = \sum_{\langle i,j\rangle\sigma} t_{\rm pd}^{ij}(d_{i\sigma}^\dagger p_{j\sigma} + {\rm H.c.}) + \sum_{\langle j,k\rangle\sigma} t_{\rm pp}^{jk}(p_{j\sigma}^\dagger p_{k\sigma} + {\rm H.c.}), \tag{2}$$

$$H_{\rm pot} = \epsilon \sum_{j\sigma} n_{j\sigma}^p + U_d \sum_i n_{i\uparrow}^d n_{i\downarrow}^d, \tag{3}$$

and

$$H_{\rm ph} = \sum_i \left(g_{cu} n_i^d + g_o \sum_{\delta'} n_{i+\delta'}^p \right) s_i^z - \Omega \sum_i s_i^x. \tag{4}$$

Here, the operator $d_{i\sigma}^\dagger$ creates a hole at a Cu $3d_{x^2-y^2}$ orbital and $p_{j\sigma}^\dagger$ creates a hole in an O2p_x or 2p_y orbital. s_i^z and s_i^x are the pseudospin operators for $S = 1/2$. U_d denotes the Coulomb energy at the Cu sites. $t_{\rm pd}^{ij} = \pm t_{\rm pd}$ and $t_{\rm pp}^{jk} = \pm t_{\rm pp}$ are the Cu-O and O-O hybridizations, respectively, with the Cu and O orbital phase factors included in the sign. The charge-transfer energy is ϵ, i.e., the oxygen orbital energy. $g_{\rm cu}$ and g_o in $H_{\rm ph}$ denote the strength of el-ph coupling. Ω stands for the tunneling frequency of the two-level system. δ' is the vector connecting Cu and its nearest-neighbor (NN) O. According to quantum cluster calculations,[21] the parameters lie in the range $t_{\rm pd} = 1.3$–1.5 eV, $t_{\rm pp} = 0.6$eV, $\epsilon = 3.6$ eV, and $U_d = 8.5$–10.5 eV. In units of $t_{\rm pd}$, we choose a parameter set $t_{\rm pp} = 0.3$ and $\epsilon = 3$, while U_d is varied from weak to strong coupling, including the physical value $U_d = 6$–8. $\Omega = 0.5$ and $g_{\rm cu} = g_o = g$ are assumed for the results presented below, except where explicitly noted otherwise.

Our calculations are performed on clusters of 2×2, 8×4, 6×6, and 8×6 unit cells with periodic boundary conditions using the ED and CPMC methods.[22,23] In the CPMC method, we follow Refs. 15 and 14 to use the Worldline representation for the pseudospins and projected the ground state $|\Psi_0\rangle$ of el-ph interacting system from a trial wave function $|\Psi_T\rangle = |\Psi_e^T\rangle \otimes |\Psi_s^T\rangle$. Here, $|\Psi_e^T\rangle$ and $|\Psi_s^T\rangle$ represent the hole and phonon parts, respectively. The CPMC algorithm has been checked against ED on the 2×2 cluster, and the difference for the electronic kinetic energy, as well as for the charge and magnetic moment at the copper sites, is less than 3% up to $U_d = 6$.

The hole binding energy is defined as

$$\Delta = E_2 + E_0 - 2E_1, \tag{5}$$

with E_n the ground-state energy for n-doped holes. The $d_{x^2-y^2}$ pairing correlation is defined by

$$P_d(\vec{R}) = \langle \Delta_d^\dagger(\vec{R}) \Delta_d(0)\rangle, \tag{6}$$

where

$$\Delta_d(\vec{R}) = \sum_{\vec{\delta}} f_d(\vec{\delta}) \{ [d_{\vec{R}\uparrow} d_{\vec{R}+\vec{\delta}\downarrow} - d_{\vec{R}\downarrow} d_{\vec{R}+\vec{\delta}\uparrow}] + [p_{\vec{R}\uparrow}^x p_{\vec{R}+\vec{\delta}\downarrow}^x - p_{\vec{R}\downarrow}^x p_{\vec{R}+\vec{\delta}\uparrow}^x] + [p_{\vec{R}\uparrow}^y p_{\vec{R}+\vec{\delta}\downarrow}^y - p_{\vec{R}\downarrow}^y p_{\vec{R}+\vec{\delta}\uparrow}^y] \}$$

with $\vec{\delta} = \pm\hat{x}, \pm\hat{y}$, $f_d(\vec{\delta}) = 1$ for $\vec{\delta} = \pm\hat{x}$ and $f_d(\vec{\delta}) = -1$ for $\vec{\delta} = \pm\hat{y}$. We calculate also the vertex contribution to the correlations defined as follows:

$$V_d(\vec{R}) = P_d(\vec{R}) - \bar{P}_d(\vec{R}), \tag{7}$$

where $\bar{P}_d(\vec{R})$ is the bubble contribution obtained with the dressed (interacting) propagator.[24]

III. RESULTS AND DISCUSSIONS

First, we show ED results for the 2×2 cluster with one hole doped beyond half filling. The electronic kinetic energy $E_k = \langle H_k\rangle$, the peak value $A^{\rm peak}$ of the single-particle spectral function $A(k,\omega)$ at the Fermi energy ($\omega = 0$), the charge $n_{\rm cu} = \langle n_i^d\rangle$, and the magnetic moment $m^2 = \langle (n_{i\uparrow}^d - n_{i\downarrow}^d)^2\rangle$ at the copper sites are displayed in Figs. 1(a)–1(d). Here, $A(k,\omega) = -\frac{1}{\pi}\sum_m \langle\Phi_0(1)|c_{m,k\sigma}(\omega - E_1 + H + i\eta)^{-1} c_{m,k\sigma}^\dagger|\Phi_0(1)\rangle$ with $\Phi_0(1)$ and E_1 denoting the ground-state wave function and its energy for one-hole doping. The index m corresponds either to the $d_{x^2-y^2}$ or to the $p_{x,y}$ orbitals, and $\eta = 0.2$. One can clearly see that E_k is lowered with increasing the el-ph coupling g at all Coulomb energies. Meanwhile, an increase of $A^{\rm peak}$ with increasing g indicates that the quasiparticle weight is increased by the el-ph coupling. In contrast, previous studies of

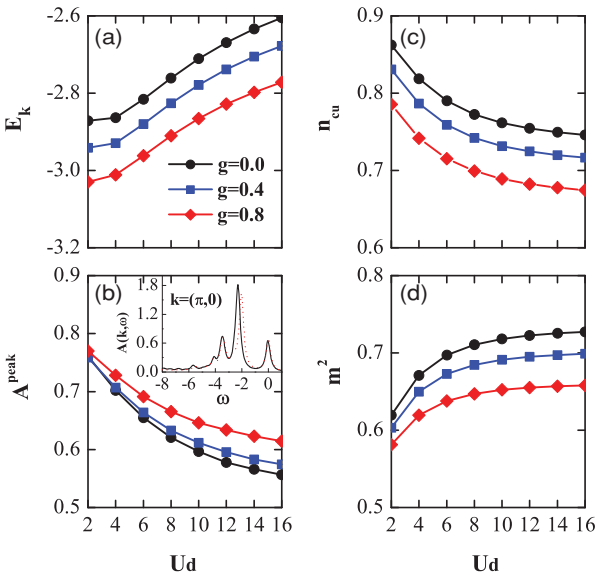

FIG. 1. (Color online) (a) Electronic kinetic energy E_k (per unit cell); (b) peak value $A^{\rm peak}$ of the spectral function $A(k = (\pi,0),\omega)$ at the Fermi energy; (c) charge $n_{\rm cu}$ and (d) magnetic moment m^2 at the copper sites as a function of U_d at different el-ph coupling g. The inset of figure (b) displays $A(k = (\pi,0),\omega)$ as a function of ω at $U_d = 6$, with $g = 0.0$ (solid line) and $g = 0.8$ (dashed line). The results are obtained from ED for the 2×2 cluster.

TABLE I. g dependence of E_k (per unit cell), $n_{\rm cu}$, m^2, and NN Cu-Cu spin correlation $\langle S_i^z \cdot S_j^z \rangle$ on the 6×6 cluster at $U_d = 6$. The number of holes $Nh = 42$, corresponding to a hole doping density $x \sim 0.167$. Statistical errors are in the last digit and are shown in parentheses.

g	E_k	$n_{\rm cu}$	m^2	$\langle S_i^z \cdot S_j^z \rangle$
0.0	−2.612(2)	0.7563(1)	0.6937(1)	−0.0800(3)
0.2	−2.659(3)	0.7426(2)	0.6786(1)	−0.0715(3)
0.4	−2.691(6)	0.7292(3)	0.6651(2)	−0.0659(6)
0.6	−2.723(9)	0.7142(5)	0.6505(5)	−0.0605(9)

harmonic phonons in the Holstein-Hubbard model found that the kinetic energy of electrons is increased with increasing el-ph coupling, accompanying a reduction of quasiparticle weight.[8,25] To explore the physical reasons for lowering E_k, we switch off the coupling of apical phonons either to copper or to in-plane oxygen, i.e., we set $g_{\rm cu} = 0$ or $g_o = 0$ in Eq. (4). It is found that E_k is lowered for the former case, but increased for the latter case. These results demonstrate that the special coupling of apical oxygen phonon to in-plane oxygen is responsible for lowering the electronic kinetic energy.

From Fig. 1(c), we notice that the charge is transferred from copper to oxygen sites, which, in combination with a phonon-mediated retarded attraction between holes with opposite spins, results in a reduction of magnetic moment at Cu sites, as shown in Fig. 1(d). Similar effects of AOP on E_k, $n_{\rm cu}$, and m^2 are also observed for larger clusters obtained by CPMC simulations, and representative results on the 6×6 cluster are shown in Table I. The last column in Table I shows that the value of NN Cu-Cu spin correlation $\langle S_i^z \cdot S_j^z \rangle$ becomes less negative with increasing g, implying a suppression of antiferromagnetic (AFM) spin correlation.

The hole binding energy Δ is shown in Fig. 2(a) as a function of the Coulomb energy U_d at different g. At all U_d, the binding energy is decreased by switching on the el-ph coupling, signaling an enhancement of hole pairing interaction. It is remarkable that this enhancement effect becomes stronger with increasing U_d, which is particularly evident in the region $U_d \leqslant 8$.

In order to identify the physical origin for this enhancement, the contributions to Δ from the hole kinetic energy E_k, the hole potential energy $E_{\rm pot} = \langle H_{\rm pot} \rangle$, and the phonon related energy $E_{\rm ph} = \langle H_{\rm ph} \rangle$ are depicted in Figs. 2(b)–2(d), respectively. Here, Δ_k, $\Delta_{\rm pot}$ and $\Delta_{\rm ph}$ have similar definitions to Δ, with E in Eq.(5) replaced with E_k, $E_{\rm pot}$ and $E_{\rm ph}$, respectively. These quantities represent the gain in the corresponding energy when the second hole is doped in the vicinity of the first one. Although the kinetic energy of holes is reduced upon increasing the el-ph coupling (see Fig. 1(a)), an increase of Δ_k with increasing g displayed in Fig. 2(b) indicates that the kinetic energy gain for two doped holes is reduced by the el-ph coupling. As seen in Fig. 2(c) and Fig. 2(d), a decrease of $\Delta_{\rm pot}$ and $\Delta_{\rm ph}$ with increasing g reveals that it is the reduction of electronic potential energy and phonon related energy between two doped holes that enhances the hole binding energy Δ. In addition, the decrease of $\Delta_{\rm pot}$ and $\Delta_{\rm ph}$ becomes more pronounced as U_d is increased, leading to a stronger enhancement of the hole binding energy in the strong correlation regime [see Fig. 2(a)].

Figure 3 displays the hole binding energy and different contributions to Δ on the 2×2 cluster with antiperiodic and mixed (periodic in the x direction and antiperiodic in the y direction) boundary conditions. A comparison of the results in Figs. 2 and 3 shows that although the boundary condition has strong effects on the amplitude of hole binding

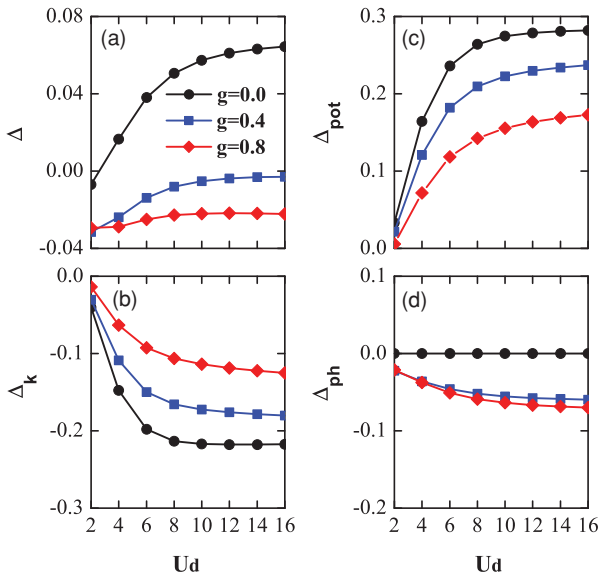

FIG. 2. (Color online) (a) Hole binding energy Δ obtained from ED for the 2×2 cluster as a function of U_d. (b)–(d) show the contributions to Δ from different energies, as discussed in text. The el-ph coupling g is indicated by the shape of the symbol.

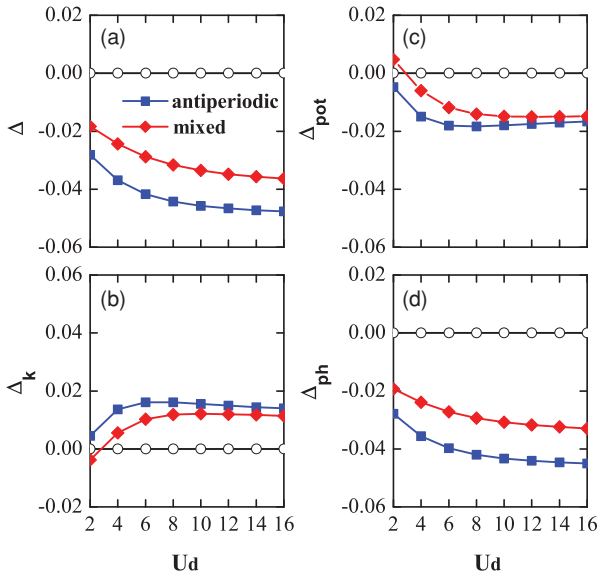

FIG. 3. (Color online) (a) Hole binding energy Δ obtained from ED for the 2×2 cluster as a function of U_d. (b)–(d) show the contributions to Δ from different energies. Open circle is for $g = 0$, and filled symbols are for $g = 0.4$ with antiperiodic (square) and mixed (diamond) boundary conditions, respectively.

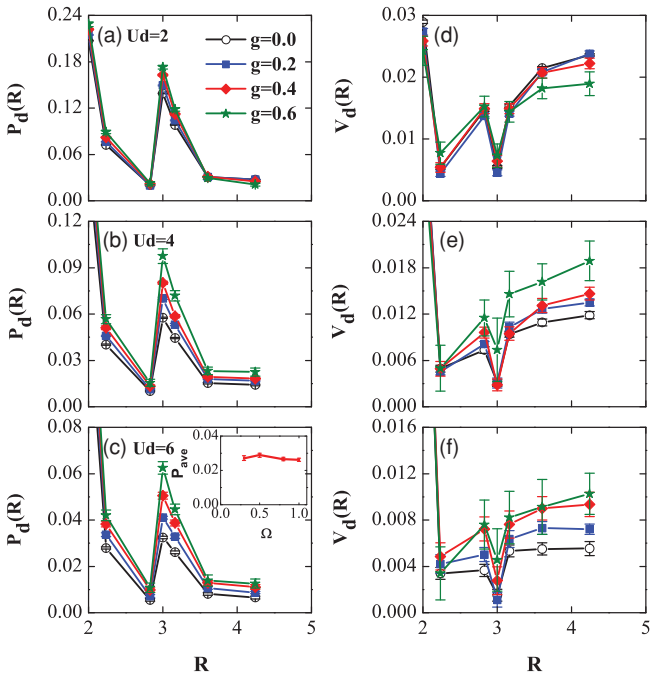

FIG. 4. (Color online) $P_d(R)$ as a function of the distance R between hole pairs on the 6×6 cluster at $U_d = 2$ (a), $U_d = 4$ (b), and $U_d = 6$ (c). (d)–(f) show the vertex contribution $V_d(R)$ corresponding to the left panels. Results are obtained for $Nh = 42$ holes. The el-ph coupling g is indicated by the shape of the symbol. The inset of figure (c) displays the average P_{ave} (see text) as a function of Ω.

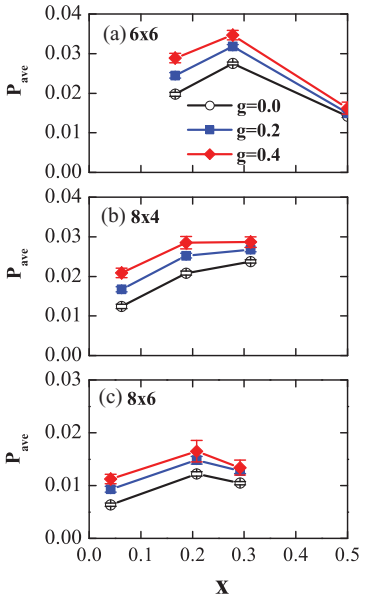

FIG. 5. (Color online) P_{ave} vs the hole doping density x for the 6×6 (a), 8×4 (b), and 8×6 (c) clusters at $U_d = 6$.

energy, the AOP-induced enhancement of hole binding energy is qualitatively similar for different boundary conditions. This demonstrates that our findings reflect the intrinsic effects of AOP in the studied model.

Based on the ED results of the small cluster, we can conclude that the coupling of AOP to holes can enhance superconductivity on the CuO_2 plane. The question arising is whether the d-wave pairing symmetry is enhanced. This issue can be addressed by examining the behavior of the d-wave pairing correlation $P_d(\vec{R})$ in Eq. (6). In Figs. 4(a)–4(c) we show $P_d(R)$ as a function of R for the 6×6 cluster at $U_d = 2$, 4, and 6, respectively. The corresponding vertex contribution is also displayed in Figs. 4(d)–4(f). In the weak-correlation case ($U_d = 2$), we observe that $P_d(R)$ is modified slightly by the el-ph coupling. However, when U_d is increased to 4 and 6, the pairing correlation is enhanced at all long-range distances for $R > 2$. At $g = 0.6$, the average enhancement of the long-range part of P_d is estimated to be about 52% and 65% for $U_d = 4$ and $U_d = 6$, respectively. This increasing enhancement of P_d with U_d is consistent with our findings for the binding energy and quasiparticle weight. A dramatic increment of the vertex contribution with increasing g, as shown in Figs. 4(e) and 4(f), further provides strong evidence that the d-wave pairing interaction is actually increased by the el-ph coupling.

We also study the effect of the tunneling frequency Ω on the pairing correlations. In the inset of Fig. 4(c), the average of long-range d-wave pairing correlation, $P_{\text{ave}} = (1/N') \sum_{R>2} P_d(\vec{R})$, where N' is the number of hole pairs with $R > 2$, is plotted as a function of Ω for $U_d = 6$ and $g = 0.4$. We notice that its frequency dependence is rather weak, suggesting that the isotope effect of apical oxygen on the superconductivity is very small. This is in good agreement with the site-selected oxygen isotope effect in $YBa_2Cu_3O_{6+x}$.[26]

To illustrate the effect of hole doping on the phonon-induced enhancement of dSC, in Fig. 5 we show P_{ave} as a function of hole doping density x at $U_d = 6$ for the 6×6, 8×4, and 8×6 clusters. The combination of the results on the three clusters shows that in a wide hole doping region $0.0 < x < 0.5$, the d-wave pairing correlation is enhanced by the el-ph coupling, and as the hole doping density is increased from underdoping to optimal doping and then to overdoping, the enhancement of P_{ave} is weakened monotonically. The reduced enhancement of P_{ave} with larger hole doping, together with the stronger enhancement of Δ and P_d with increasing U_d, demonstrates that strong electronic correlations and/or AFM fluctuations play a crucial role in the phonon-induced enhancement of dSC.

IV. CONCLUSIONS

In summary, our numerical simulations show that the hole binding energy is strongly enhanced by an AOP-induced reduction of electronic potential energy and phonon related energy. As a combination of two concurring effects, i.e., the enhancement of hole pairing interaction and the increase of quasiparticle weight, the long-range part of d-wave pairing correlations is dramatically enhanced with increasing the el-ph coupling strength. Our results also show that strong electronic correlations and/or AFM fluctuations are crucial for this phonon-induced enhancement effect. The consistent behavior of our results on different clusters suggests that the phonon-induced enhancement of dSC could survive in the thermodynamic limit.

ACKNOWLEDGMENTS

We thank W. Hanke, F. F. Assaad, and A. S. Mishchenko for enlightening discussions. This work was supported by NSFC under Grants No. 10674043 and No. 10974047. H.Q.L. acknowledges support from HKRGC 402109. E.A. was supported by the Austrian Science Fund (FWF) under Grant No. P18551-N16.

[1] L. Pintschovius, Phys. Status Solidi B **242**, 30 (2005).

[2] L. Pintschovius, D. Reznik, and K. Yamada, Phys. Rev. B **74**, 174514 (2006).

[3] A. Lanzara, P. V. Bogdanov, X. J. Zhou, S. A. Keller, D. L. Feng, E. D. Lu, T. Yoshida, H. Eisaki, A. Fujimori, K. Kishio, J.-I. Shimoyama, T. Noda, S. Uchida, Z. Hussain, and Z.-X. Shen, Nature (London) **412**, 510 (2001).

[4] T. Cuk, F. Baumberger, D. H. Lu, N. Ingle, X. J. Zhou, H. Eisaki, N. Kaneko, Z. Hussain, T. P. Devereaux, N. Nagaosa, and Z.-X. Shen, Phys. Rev. Lett. **93**, 117003 (2004).

[5] Z. B. Huang, W. Hanke, E. Arrigoni, and D. J. Scalapino, Phys. Rev. B **68**, 220507(R) (2003).

[6] C. Honerkamp, H. C. Fu, and D. H. Lee, Phys. Rev. B **75**, 014503 (2007).

[7] L. Vidmar, J. Bonca, S. Maekawa, and T. Tohyama, Phys. Rev. Lett. **103**, 186401 (2009).

[8] A. Macridin, B. Moritz, M. Jarrell, and T. Maier, Phys. Rev. Lett. **97**, 056402 (2006).

[9] J. A. Slezak, J. H. Lee, M. Wang, K. McElroy, K. Fujita, B. M. Andersen, P. J. Hirschfeld, H. Eisaki, S. Uchida, and J. C. Davis, Proc. Natl. Acad. Sci. USA **105**, 3203 (2008).

[10] H. Hobou, S. Ishida, K. Fujita, M. Ishikado, K. M. Kojima, H. Eisaki, and S. Uchida, Phys. Rev. B **79**, 064507 (2009).

[11] W. B. Gao, Q. Q. Liu, L. X. Yang, Y. Yu, F. Y. Li, C. Q. Jin, and S. Uchida, Phys. Rev. B **80**, 094523 (2009).

[12] M. Merz, N. Nucker, P. Schweiss, S. Schuppler, C. T. Chen, V. Chakarian, J. Freeland, Y. U. Idzerda, M. Klaser, G. Muller-Vogt, and Th. Wolf, Phys. Rev. Lett. **80**, 5192 (1998).

[13] M. Mori, G. Khaliullin, T. Tohyama, and S. Maekawa, Phys. Rev. Lett. **101**, 247003 (2008); E. Pavarini, I. Dasgupta, T. Saha-Dasgupta, O. Jepsen, and O. K. Andersen, *ibid*. **87**, 047003 (2001).

[14] M. Frick, I. Morgenstern, and W. von der Linden, Z. Phys. B **82**, 339 (1991).

[15] M. Frick, W. von der Linden, I. Morgenstern, and H. de Raedt, Z. Phys. B **81**, 327 (1990).

[16] D. Haskel, E. A. Stern, D. G. Hinks, A. W. Mitchell, and J. D. Jorgensen, Phys. Rev. B **56**, R521 (1997).

[17] S. D. Conradson, I. D. Raistrick, and A. R. Bishop, Science **248**, 1394 (1990).

[18] J. Mustre de Leon, S. D. Conradson, I. Batistic, and A. R. Bishop, Phys. Rev. Lett. **65**, 1675 (1990).

[19] N. M. Plakida, Phys. Scr. T **29**, 77 (1989).

[20] N. M. Plakida, V. L. Aksenov, and S. L. Drechsler, Europhys. Lett. **4**, 1309 (1987).

[21] R. L. Martin, Phys. Rev. B **53**, 15501 (1996).

[22] Z. B. Huang, H. Q. Lin, and J. E. Gubernatis, Phys. Rev. B **63**, 115112 (2001).

[23] S. W. Zhang, J. Carlson, and J. E. Gubernatis, Phys. Rev. Lett. **74**, 3652 (1995); Phys. Rev. B **55**, 7464 (1997).

[24] S. R. White, D. J. Scalapino, R. L. Sugar, N. E. Bickers, and R. T. Scalettar, Phys. Rev. B **39**, 839 (1989).

[25] G. Sangiovanni, O. Gunnarsson, E. Koch, C. Castellani, and M. Capone, Phys. Rev. Lett. **97**, 046404 (2006).

[26] D. Zech, H. Keller, K. Conder, E. Kaldis, E. Liarokapis, N. Poulakis, and K. A. Muller, Nature (London) **371**, 681 (1994).